Fracture Mechanics of Concrete and Concrete Structures -
Recent Advances in Fracture Mechanics of Concrete - B. H. Oh, et al.(eds)

Snap-through cracking in plastic concrete slabs

P.H. Morris, P.F. Dux & V.T.N. Dao
The University of Queensland, Brisbane, Australia

ABSTRACT: Snap-through cracking of desiccating plastic concrete slabs, which is occasionally observed in practice, can reduce significantly the service life of concrete structures. However, its underlying mechanism has remained largely unexplained, with very limited literature available. In this paper, theoretical analyses of snap-through cracking in plastic concrete slabs, which are based on combined geotechnical engineering and fracture mechanics models, are presented. The results obtained capture the essential features of snap-through cracking, showing how surface cracks in plastic concrete can become unstable, deepen rapidly, and either become stable again or propagate through the full depth of the slab. They also clarify the roles and significance of pre-existing surface cracks and surface defects, pore moisture suction, and the depth of desiccation in this process. Most importantly, they also confirm the critical role of good construction practices, including the control of compaction and desiccation, in preventing this form of cracking.

1 INTRODUCTION

Snap-through cracking is the term used in this paper to describe the sudden and almost instantaneous growth to considerably greater depths of apparently stable, relatively shallow cracks in the exposed surface of concrete slabs. This often occurs under essentially constant loading, and, in the most extreme cases, the cracks extend completely through the slab. In plastic concrete, the cracking is driven primarily by the pore moisture suction (negative pore pressure) associated with desiccation of the concrete (Cohen et al. 1990, Morris & Dux 2006, Dao 2007).

The economic consequences of snap-through cracking in plastic concrete, which can dramatically impair the serviceability of concrete structures, can be very severe. Even cracks that are initially relatively short can deepen and lengthen considerably even after the concrete has matured (Uno 1998), promoting the ingress of deleterious materials and subsequent deterioration. It is thus important that the underlying mechanism be well understood.

Snap through cracking is occasionally observed in plastic concrete and has also been observed in mature concrete (Crisfield 1986), clay soils (Morris et al. 1992, Morris et al. 1994), and brittle elastic solids (Nemat-Nasser et al. 1980), yet despite this, has received relatively little attention amongst engineering researchers and practitioners. Snap-through cracking in plastic concrete was first considered by Morris and Dux (2003). However, they considered only linear suction profiles in semi-infinite slabs, and their analysis was restricted by the very limited availability of material parameter data.

In this paper, theoretical analyses of snap-through cracking in plastic concrete slabs are presented that are based on a combined geotechnical engineering (particulate material)–fracture mechanics failure model. While the simplified analyses presented here rely on the Irwin-Orowan extension of linear elastic fracture mechanics to ductile materials (Irwin & Kies 1952, Orowan 1955) and do not consider the dynamics of rapid crack propagation, they nevertheless capture the essential features of snap-through cracking, showing how initially shallow cracks in plastic concrete can become unstable and deepen suddenly. They also clarify the roles of suction, various engineering material parameters, and surface defects in this process.

2 SOLUTIONS FOR CRACK DEPTH

Cracks in plastic concrete tend to propagate by opening along their own axes and are often essentially planar over significant distances relative to the depth of the crack. In terms of the three fundamental modes of fracture mechanics, they are thus Mode I cracks. (Modes II and III respectively involve shearing and tearing parallel to the crack axis.) The following analyses consider only a single Mode I vertical crack in plane strain (Fig. 1). The crack propagates downwards from the surface of the concrete without interacting with other, nearby cracks.

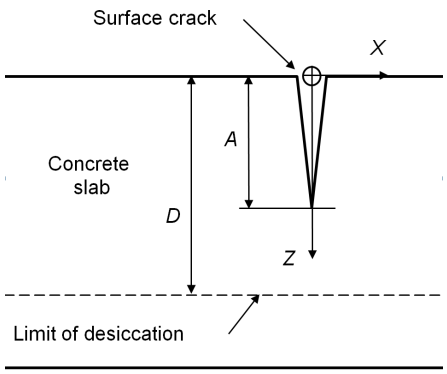

Figure 1. Definition sketch of concrete slab.

Within the limitations of linear elastic fracture mechanics, the crack depth for the given loading and geometry can be determined by simply equating the fracture toughness, which is a function of several material parameters, and the calculated stress intensity factor, which is a function of the crack geometry and the stress distribution within the concrete. Numerous solutions are available for simple stress distributions and crack geometries, and the rules for combining them are well known (Meguid 1989, Wu & Carlsson 1991). Here stress intensity factors are calculated using the very versatile weight function method (Bueckner 1970, Rice 1972, Wu & Carlsson 1991).

2.1 *Stresses in cracked plastic concrete*

To determine crack depths using the weight function method, it is necessary initially to calculate the stresses in the plastic concrete adjacent to the crack. The approach adopted was to invoke Bueckner's principle (Bueckner 1958), which states that the stress intensity factor for a stress-free crack (i.e. one with no loads on the crack faces) in a loaded body is identical with that for the same crack loaded internally with the stresses required to produce zero relative strain at the crack faces under the original loading. Since, in the simplified fracture mechanics model adopted, cracks are assumed to be stress-free, the problem of calculating the stresses adjacent to the crack is thus reduced to calculating the stresses at the crack location in an equivalent uncracked body.

Bueckner's principle, however, is inapplicable to problems in which the crack affects potential distributions, for example, a crack that is parallel to the direction of pore moisture flow (Morris et al. 1994). Consequently, it is applicable to cracks in plastic concrete only if the cracks do not affect the distribution of suctions (or pore moisture pressures) therein. The following analyses consider concrete slabs in which suctions are functions only of the depth below the slab surface. In real slabs, evaporation and flow of pore moisture from the crack faces as well as normal variability cause the suctions to vary in plan as well as with depth.

Total stresses are considered, and all stresses and pressures, including suctions, are based on the atmospheric datum (i.e. atmospheric pressure taken as zero) (Morris & Dux 2005). The usual convention of geotechnical engineering is followed; that is, compressive inter-particle stresses and pore pressures are taken as positive. However, although suctions are negative pore pressures, for convenience they too are taken as numerically positive. No distinction is drawn between the effects of matric and osmotic suction (Morris & Dux 2005), although the effects of the latter in plastic concrete remain uncertain (Dao et al. 2005). Desiccation due to hydration and the associated matric suction are, unless noted otherwise, assumed to be negligible.

It is also assumed that the stress due to the pore moisture suction is equal to the suction. This is true only if the concrete is saturated or almost saturated (Morris & Dux 2003, Morris & Dux 2006). It is not, however, critical to the outcome of the analyses. The significance of the surface suction in the analyses is discussed further below.

It is assumed that the concrete is isotropic and elastic and remains so even if the strains are forced to be one-dimensional. The horizontal strain perpendicular to the crack (Fig. 1) is then given by (Morris et al. 1992):

$$\varepsilon_X = \frac{\sigma_X}{E} - \frac{\nu}{E}(\sigma_Y + \sigma_Z) - \frac{u_w}{H} \qquad (1)$$

where ε_X = horizontal strain perpendicular to crack; σ_X = horizontal normal stress perpendicular to crack, Pa; E = Young's modulus of plastic concrete for normal stress, Pa; ν = Poisson's ratio of plastic concrete; σ_Y = horizontal normal stress parallel to crack, Pa; σ_Z = vertical normal stress, Pa; u_w = pore moisture pressure, Pa; and H = Young's modulus of plastic concrete for pore moisture pressure and suction, Pa.

Separate Young's moduli are defined in Equation (1) for the responses of the plastic concrete to normal stresses and to pore moisture pressures and suctions because it has not yet been established that a single modulus is sufficient (Morris et al. 1992). If the concrete reacts in the same way to normal stresses and the essentially isotropic pore moisture pressures and suctions (Morris et al. 1992):

$$\frac{E}{H} = 1 - 2\nu \qquad (2)$$

Prior to cracking, the stresses and strains in the concrete are essentially one-dimensional. That is, the normal stresses perpendicular and parallel to the

crack are equal and the corresponding strains are both zero. Combining Equations (1) and (2) then gives:

$$\sigma_X = \left(\frac{\nu}{1-\nu}\right)\sigma_Z + \left(\frac{1-2\nu}{1-\nu}\right)u_w \quad (3)$$

For depths less than the depth of desiccation (at which, by definition, the suction is zero) Equation (3) becomes:

$$\sigma_X = \left(\frac{\nu}{1-\nu}\right)\gamma_d Z - \left(\frac{1-2\nu}{1-\nu}\right)\Psi_Z \quad (4)$$

where Z = depth below surface of slab, m; Ψ_Z = suction at depth Z below surface of slab, Pa; and γ_d = unit weight of desiccated concrete, N/m^3.

For depths greater than the depth of desiccation, Equation (3) becomes:

$$\sigma_X = \left(\frac{\nu}{1-\nu}\right)\left(\gamma_d D + \gamma_s (Z-D)\right) - \left(\frac{1-2\nu}{1-\nu}\right)\gamma_w (Z-D) \quad (5)$$

where γ_s= unit weight of saturated concrete, N/m^3; γ_w = unit weight of pore moisture, N/m^3; and D = depth of desiccation, m.

2.2 *Suction profiles*

A uniform suction profile over the full depth of the slab was initially considered. The depth of desiccation is equal to the thickness of the slab in this case. The uniform profile represents low (45 mm ± 10 mm) slump concrete that is desiccated both prior to and immediately following placement, before evaporation from the exposed upper surface becomes significant. Such concretes are often used in highway slabs to minimize the requirement for formwork. Osmotic suction due to dissolved salts in the pore moisture can contribute significantly to the initial suction (Morris & Dux 2003), but, as noted above, might not affect crack propagation (Dao et al. 2005, Morris & Dux 2006). Also, in this case only, the matric suction due to hydration, which can be considered uniform throughout the slab, can be assumed to contribute to the total suction affecting crack propagation without changing the analysis.

In addition, the following power function suction profiles (Fig. 2) for depths less than the depth of desiccation (Fig. 1) were considered:

$$\Psi_Z = \Psi_0\left(1 - \frac{Z}{D}\right)^g \quad (6)$$

where Ψ_0 = suction at surface of slab, Pa; and g = exponent of suction profile.

Below the depth of desiccation, the pore pressure (a negative suction) is hydrostatic. That is,

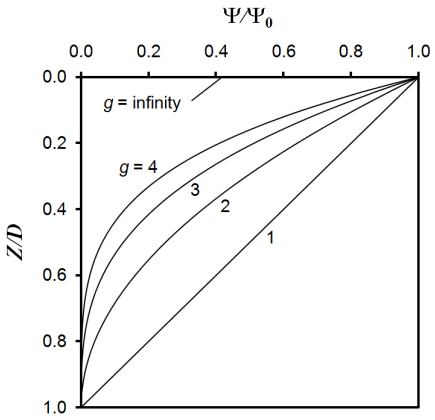

Figure 2. Suction profiles above depth of desiccation.

$$\Psi_Z = -\gamma_w (Z-D) \quad (7)$$

Equations (6) and (7) are together reasonably representative of the suction profiles that develop in initially saturated concrete desiccating monotonically from an exposed surface (Fig. 2) (Morris & Dux 2005). If the surface of the slab is fully desiccated, the suction at the surface will equal the atmospheric suction, while, as noted above, the matric suction at the depth of desiccation equals zero, corresponding to 100% saturation.

The exponent g in Equation (6) can assume values ranging from unity to infinity (Fig. 2). A value of infinity corresponds to the limiting profile with a finite suction value at the exposed surface of the concrete and zero suction over the remainder of the profile. A value of unity corresponds to a linear suction profile. A g value close to four, which corresponds to con-cave quartic suction profiles, probably best reflects ordinary on-site conditions.

2.3 *Variation of stress intensity factor with depth*

Analytical expressions for the stress intensity factor as a function of the crack depth have been obtained for finite and semi-infinite slabs for crack depths both less and greater than the depth of desiccation. However, the expressions for semi-infinite slabs for crack depths greater than the depth of desiccation and for all finite slabs are much too lengthy to present here.

The expressions for semi-infinite slabs for crack depths less than the depth of desiccation (Fig. 1) are, however, relatively simple. Those for the uniform, linear, and concave quartic suction profiles (Fig. 2) are, respectively:

$$K = 1.9878\left(\frac{1-2\nu}{1-\nu}\right)\Psi_0 A^{0.5} - 1.2088\left(\frac{\nu}{1-\nu}\right)\gamma_d A^{1.5} \quad (8)$$

$$K = 1.9878\left(\frac{1-2\nu}{1-\nu}\right)\Psi_0 A^{0.5} - 1.2088\left(\left(\frac{1-2\nu}{1-\nu}\right)\frac{4\Psi_0}{D} + \left(\frac{\nu}{1-\nu}\right)\gamma_d\right)A^{1.5} \quad (9)$$

and

$$K = 1.9878\left(\frac{1-2\nu}{1-\nu}\right)\Psi_0 A^{0.5} - 1.2088\left(\left(\frac{1-2\nu}{1-\nu}\right)\frac{4\Psi_0}{D} + \left(\frac{\nu}{1-\nu}\right)\gamma_d\right)A^{1.5} + 5.5778\left(\frac{1-2\nu}{1-\nu}\right)\frac{\Psi_0}{D^2}A^{2.5} - 3.1195\left(\frac{1-2\nu}{1-\nu}\right)\frac{\Psi_0}{D^3}A^{3.5} + 0.6840\left(\frac{1-2\nu}{1-\nu}\right)\frac{\Psi_0}{D^4}A^{4.5} \quad (10)$$

2.4 *Fracture toughness*

To obtain solutions for the crack depth, it remains only to determine the fracture toughness (critical stress intensity factor) for the concrete in question. For cracking in plane strain, the fracture toughness is given by (Irwin 1957, Meguid 1989):

$$K_{cr} = \sqrt{\frac{2G_F E}{1-\nu^2}} \quad (11)$$

where K_{cr} = fracture toughness for Mode I cracking, N/m$^{3/2}$; and G_F = specific fracture energy, J/m^2.

The fracture toughness of plastic concrete is thus a function of its Young's modulus, Poisson's ratio, and specific fracture energy, which are all functions of the degree of hydration (De Schutter & Taerwe 1996, Morris & Dux 2005, Dao et al. 2009). Consequently, anything that affects the rate of hydration, such as the use of admixtures or the temperature of the concrete, will also affect the development of snap-through cracking. Unfortunately, no correlations exist for the fracture toughness with any well-known concrete parameter such as, for example, the 28-day compressive strength.

2.5 *Input parameter values*

The primary input parameters required to determine crack depths using the equations discussed above are the fracture toughness and Poisson's ratio of plastic concrete, the bulk densities of saturated and desiccated concrete and the pore moisture, the suction at the surface of the concrete, and the depth of desiccation.

No data are available for the fracture toughness of plastic concrete. However, it can be estimated using Equation (11) and existing data for the Young's modulus, Poisson's ratio, and specific fracture energy of plastic concrete. It has been shown in tensile strength tests that the Young's modulus of plastic concrete increases with time and may reach about 600 MPa at 6.5 h after mixing (Dao et al. 2009). Values up 28000 MPa have also been recorded at 12 h (Oluokun et al. 1991, Kovler 1994). The Young's modulus of plastic cement paste varies from 0 MPa initially to about 10 MPa at 8 h (Boumiz et al. 1996).

The Poisson's ratio of concrete decreases from 0.5 immediately after mixing to about 0.2 when the degree of hydration reaches 10% (Ouldhammou et al. 1990, Oluokun et al. 1991, De Schutter & Taerwe 1996). The Poisson's ratio of plastic cement pastes similarly varies from 0.49 to 0.28 (Boumiz et al. 1996).

The specific fracture energy of plastic concrete increases with increasing time, reaching about 80 J/m^2 at 6.5 h after mixing (Dao et al. 2009). The specific fracture energy of plastic cement mortars at ages from 2.2 h to 6.4 h assumes a similar range of values (Morris & Dux 2005).

On the basis of the foregoing, representative values of 70 MPa, 0.30, and 16 J/m^2 were adopted for the Young's modulus, Poisson's ratio, and specific fracture energy of plastic concrete, respectively. These three values together correspond to a fracture toughness of approximately 50 kN/m$^{3/2}$ (Eq. (11)). This is comparable to the fracture toughness of mature concrete, which typically ranges from 50 kN/m$^{3/2}$ to 100 kN/m$^{3/2}$ (Carpinteri 1981, Crisfield 1986, Bosco et al. 1990). However, because the Young's modulus of plastic concrete increases rapidly with increasing age (Dao et al. 2009), considerably higher values of fracture toughness are clearly possible.

In the absence of experimental data on the effects of desiccation on the density of plastic concrete, a value of 23 kN/m^3 was used for both saturated and unsaturated concrete. The density of the pore moisture was taken as 10 kN/m^3.

The solutions for crack depth were based on values for the suction at the surface of the concrete of 0.5 MPa and 5 MPa for low slump and normal slump concrete, respectively. These suction values are based on limited but reasonably representative laboratory data obtained using a pychrometer and a leaf hygrometer. At 20 ^{o}C, they correspond to relative humidities in the pores in the concrete of 99.6 % and 96.4 %, respectively (Philip 1957, Morris & Dux 2005). They are significantly lower than typical atmospheric suctions, which can readily reach values approaching 100 MPa or even more (Morris & Dux 2005, Morris & Dux 2006).

Depths of desiccation of 2 mm, 6 mm, and 10 mm were considered. For initially saturated concrete with the representative void ratio (volume of voids divided by volume of solids) of 0.2, and a constant, very high evaporation rate of 2 kg/m^2/h (ACI Committee 308 2001), these values correspond to delays of 12 min, 36 min, and 60 min following the evaporation of the last of the bleed water, if any, to empty the voids completely. It is thus unlikely but not impossible that a depth of desiccation of 10 mm will be reached in practice, but a depth of 2 mm or more could be reached easily.

3 SOLUTIONS FOR SNAP-THROUGH CRACKING

The solutions for crack depth based on the foregoing analyses are presented in Figures 3 to 6 for slabs ranging in thickness from 100 mm to 1200 mm and semi-infinite slabs. The solutions are presented and discussed initially only in terms of the representative values of fracture toughness (50 kN/m$^{3/2}$) and (0.5 MPa and 5 MPa) nominated above. However, Figures 3 to 6 can be used to obtain solutions for a wide range of such input values by simple geometric scaling.

3.1 *Solutions for uniform suction profile*

Figure 3 shows the solutions for stress intensity factor corresponding to uniform suction of 0.5 MPa over the full depth of the slab, which, as noted above, represents a low slump concrete immediately after placing. For all slab depths, the stress intensity factor increases monotonically with increasing crack depth. Cracks with depths that correspond to stress intensity factor less than the fracture toughness of 50 kN/m$^{3/2}$ will remain stable; deeper cracks will experience snap-through propagation through the full thickness of the slab. For the parameter values considered, the latter correspond in all cases to a crack depth of approximately 8 mm or more (Fig. 3).

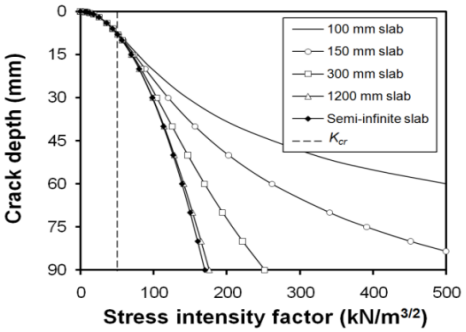

Figure 3. Variation of stress intensity factor with crack depth for uniform suction of 0.5 MPa over full depth of slab.

3.2 *Solutions for concave quartic suction profiles*

Figures 4 to 6 show the solutions for crack depth corresponding to concave quartic suction profiles (Fig. 2) with 5 MPa surface suction and depths of desiccation of 2 mm, 6 mm, and 10 mm respectively. As noted above, these profiles represent normal slump concrete that is allowed to desiccate from the exposed surface after placing.

Unlike for the case of uniform suction profile (Fig. 3), however, the stress intensity factors in Figures 4 to 6 do not increase monotonically with crack depth. This is primarily attributable to the shallow depths of desiccation and is of great significance for the behavior of cracks and pre-existing defects. Comparison of the three figures shows that, although the overall form of the solutions does not change, the crack depths corresponding to a given stress intensity factor increase with increasing depth of desiccation. That is, the solutions confirm that the severity of the conditions promoting snap-through cracking increases with the depth of desiccation.

Figure 4 shows that for a depth of desiccation of 2 mm and the other input values considered, the stress intensity factor of surface cracks or defects approximately 0.1 mm in depth exceeds the fracture toughness. Consequently, surface cracks or defects of that size or larger will experience snap-through propagation. For all slabs, however, the stress intensity factor falls below the critical value of 50 kN/m$^{3/2}$ for cracks deeper than approximately 1.5 mm. Snap-through propagation consequently stops at this depth and will not resume unless either the surface suction, the depth of desiccation, or both increase. However, the stress intensity factor for the 100 mm slab again exceeds the fracture toughness for surface cracks or defects that are 61 mm or deeper. Any of the latter will thus experience snap-through cracking through the full depth of the slab. Deeper cracks or defects are necessary to produce the same result in the thicker slabs.

The solutions for depths of desiccation of 6 mm (Fig. 5) and 10 mm (Fig. 6) are similar to those for the 2 mm depth (Fig. 4). Very small surface defects can, however, cause snap-through cracking of the full thickness of the 100 mm slab for depths of desiccation of 6 mm and of the 100 mm and 150 mm slabs for depths of desiccation of 10 mm. Also, the depth of crack or defect that will cause full-depth snap-through cracking of the thicker slabs, although relatively large, decreases as the depth of desiccation increases.

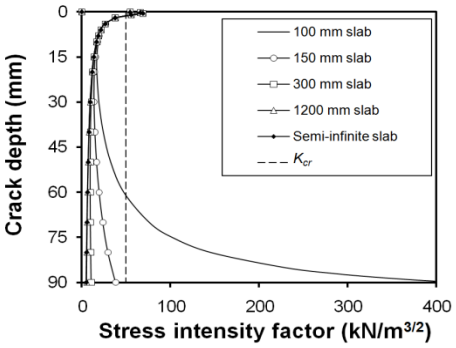

Figure 4. Variation of stress intensity factor with crack depth for concave quartic suction profile over uppermost 2 mm depth of slab and 5 MPa suction at surface.

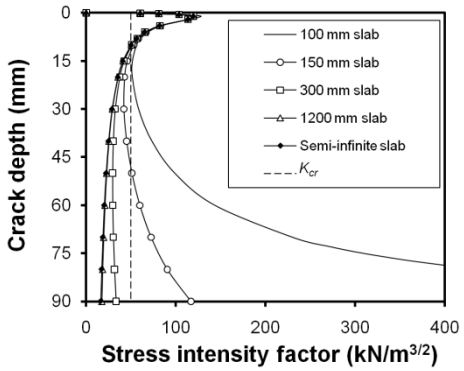

Figure 5. Variation of stress intensity factor with crack depth for concave quartic suction profile over uppermost 6 mm depth of slab and 5 MPa suction at surface.

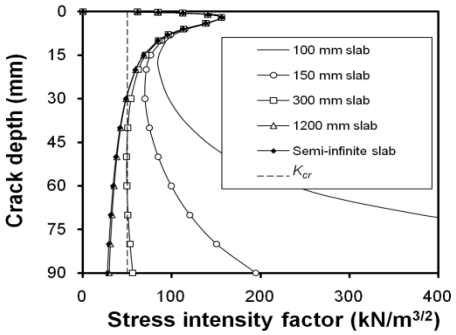

Figure 6. Variation of stress intensity factor with crack depth for concave quartic suction profile over uppermost 10 mm depth of slab and 5 MPa suction at surface.

4 SUMMARY AND CONCLUSIONS

Analytical solutions for the depth of cracking in desiccating plastic concrete slabs have been described in which it is assumed that plastic concrete is a frictional particulate material that can be characterized using geotechnical engineering principles and that the cracking is driven by pore moisture suction. Suction profiles that are representative of low and normal slump concretes were considered.

It has been clearly demonstrated that the solutions presented (Figs. 3 to 6) capture the essential features of snap-through cracking, showing how surface cracks in plastic concrete can become unstable, deepen rapidly, and either become stable again or propagate through the full depth of the slab. They also clarify the roles and significance of pre-existing surface cracks and surface defects, pore moisture suction, and the depth of desiccation in this process. Most importantly, they also confirm the critical role of good construction practices, including primarily the control of compaction and desiccation, in preventing it.

However, because of the simplifications adopted, including notably the use of linear elastic rather than elasto-plastic fracture mechanics, and the limited input data available, the results obtained should be considered semi-quantitative only. Further work is being carried out by the authors to improve them.

REFERENCES

ACI Committee 308 2001. *Guide to Curing Concrete (ACI 308R-01)*. American Concrete Institute.

Bocca, P. et al. 1991. Mixed mode fracture of concrete. *International Journal of Solids and Structures* 27(9): 1139-1153.

Boumiz, A. et al. 1996. Mechanical properties of cement pastes and mortars at early ages. *Advanced Cement Based Materials* 3(3-4): 94-106.

Bueckner, H.F. 1958. The Propagation of Cracks and the Energy of Elastic Deformation. *Transactions of the American Society of Mechanical Engineers* 80E: 1225-1230.

Bueckner, H.F. 1970. A novel principle for the computation of stress intensity factors. *Zeit-schrift fur Angewandte Mathematik und Mechanik* 50(9): 529-546.

Carpinteri, A. 1981. Static and Energetic Fracture Parameters for Rocks and Concretes. *Materials and Structures* 14(81): 151-162.

Cohen, M.D. et al. 1990. Mechanism of plastic shrinkage cracking in portland cement and portland cement-silica fume paste and mortar. *Cement and Concrete Research* 20(1): 103-119.

Crisfield, M.A. 1986. Snap-Through and Snap-Back Response in Concrete Structures and the Dangers of Under-Integration. *International Journal for Numerical Methods in Engineering* 22(3): 751-767.

Dao, V.N.T. 2007. *Early-age cracking of concrete*. Brisbane: University of Queensland, Australia.

Dao, V.N.T. et al. 2005. Plastic cracking of concrete: The roles of osmotic and matric suctions. In R.K. Dhir et al. (eds), *Cement combinations for durable concrete-Proceedings of the International Conference on "Global construction: Ultimate concrete opportunities"*, 407-416. Dundee: Thomas Telford.

Dao, V.N.T. et al. 2009. Tensile properties of early-age concrete. *ACI Materials Journal* 106(6): 1-10.

De Schutter, G. & Taerwe, L. 1996. Degree of hydration-based description of mechanical properties of early age concrete. *Materials and Structures/Materiaux et Constructions* 29(190): 335-344.

Irwin, G.R. & Kies, J.A. 1952. Fracturing and fracture dynamics. *Welding Journal* 31(2): 95-100.

Irwin, G.R. 1957. Analysis of stresses and strains near the end of a crack traversing a plate. *Journal of Applied Mechanics* 24: 361-364.

Kovler, K. 1994. Testing system for determining the mechanical behaviour of early age concrete under restrained and free uniaxial shrinkage. *Materials and Structures/Materiaux et Constructions* 27(170): 324-330.

Meguid, S.A. 1989. *Engineering fracture mechan-ics*. London: Elsevier.

Morris, P.H. & Dux, P.F. 2003. Cracking of plastic concrete. *Australian Journal of Civil Engineering* 1(1): 17-21.

Morris, P.H. & Dux, P.F. 2005. Suctions, fracture energy, and plastic cracking of cement mortar and concrete. *ACI Materials Journal* 102(6): 390-396.

Morris, P.H. & Dux, P.F. 2006. Crack depths in desiccating plastic concrete. *ACI Materials Journal* 103(2): 90-96.

Morris, P.H. et al. 1992. Cracking in drying soils. *Canadian Geotechnical Journal* 29: 263-277.

Morris, P.H. et al. 1994. Crack depths in drying clays using fracture mechanics. *ASCE Geotechnical* Special Publication No. 43: 40-537.

Nemat-Nasser, S. et al. 1980. Unstable growth of tension cracks in brittle solids: Stable and unstable bifurcations, snap-through, and imperfection sensitivity. *International Journal of Solids and Structures* 16(11): 1017-35.
Orowan, E. 1955. Energy criteria of fracture. *Welding Journal* 34(3): 157-160.
Oluokun, F.A. et al. 1991. Elastic modulus, Poisson's ratio, and compressive strength relationships at early ages. *ACI Materials Journal* 88(1): 3-10.
Ouldhammou, L. et al. 1990. Mechanical properties of fresh concrete before setting. In P.F.G. Banfill (ed), *Rheology of Fresh Cement and Concrete*: 249-258. Liverpool: E. & F.N. Spon.
Philip, J.R. 1957. Evaporation, and moisture and heat fields in the soil. *Journal of Meteorology* 14: 354-366.
Rice, J.R. 1972. Some remarks on elastic crack-tip stress fields. *International Journal of Solids and Structures* 8(6): 751-8.
Uno, P.J. 1998. Plastic shrinkage cracking and evaporation formulas. *ACI Materials Journal* 95(4): 365-375.
Wu, X.R. & Carlsson, A.J. 1991. *Weight Functions and Stress Intensity Factor Solutions*. Oxford: Pergamon.